OPEN

Residual Myocardial Iron Following Intramyocardial Hemorrhage During the Convalescent Phase of Reperfused ST-Segment–Elevation Myocardial Infarction and Adverse Left Ventricular Remodeling

Heerajnarain Bulluck, MBBS; Stefania Rosmini, MD, PhD; Amna Abdel-Gadir, MBBS; Steven K. White, MBChB; Anish N. Bhuva, MBBS; Thomas A. Treibel, MBBS; Marianna Fontana, MD, PhD; Manish Ramlall, MBChB; Ashraf Hamarneh, MBBS; Alex Sirker, PhD; Anna S. Herrey, MD, PhD; Charlotte Manisty, PhD; Derek M. Yellon, MSc, PhD; Peter Kellman, PhD; James C. Moon, MD; Derek J. Hausenloy, PhD

Background—The presence of intramyocardial hemorrhage (IMH) in ST-segment–elevation myocardial infarction patients reperfused by primary percutaneous coronary intervention has been associated with residual myocardial iron at follow-up, and its impact on adverse left ventricular (LV) remodeling is incompletely understood and is investigated here.

Methods and Results—Forty-eight ST-segment–elevation myocardial infarction patients underwent cardiovascular magnetic resonance at 4±2 days post primary percutaneous coronary intervention, of whom 40 had a follow-up scan at 5±2 months. Native T1, T2, and T2* maps were acquired. Eight out of 40 (20%) patients developed adverse LV remodeling. A subset of 28 patients had matching T2* maps, of which 15/28 patients (54%) had IMH. Eighteen of 28 (64%) patients had microvascular obstruction on the acute scan, of whom 15/18 (83%) patients had microvascular obstruction with IMH. On the follow-up scan, 13/15 patients (87%) had evidence of residual iron within the infarct zone. Patients with residual iron had higher T2 in the infarct zone surrounding the residual iron when compared with those without. In patients with adverse LV remodeling, T2 in the infarct zone surrounding the residual iron was also higher than in those without (60 [54–64] ms versus 53 [51–56] ms; *P*=0.025). Acute myocardial infarct size, extent of microvascular obstruction, and IMH correlated with the change in LV end-diastolic volume (Pearson's rho of 0.64, 0.59, and 0.66, respectively; *P*=0.18 and 0.62, respectively, for correlation coefficient comparison) and performed equally well on receiver operating characteristic curve for predicting adverse LV remodeling (area under the curve: 0.99, 0.94, and 0.95, respectively; *P*=0.19 for receiver operating characteristic curve comparison).

Conclusions—The majority of ST-segment–elevation myocardial infarction patients with IMH had residual myocardial iron at follow-up. This was associated with persistently elevated T2 values in the surrounding infarct tissue and adverse LV remodeling. IMH and residual myocardial iron may be potential therapeutic targets for preventing adverse LV remodeling in reperfused ST-segment–elevation myocardial infarction patients. **(*Circ Cardiovasc Imaging*. 2016;9:e004940. DOI: 10.1161/CIRCIMAGING.116.004940.)**

Key Words: cardiovascular magnetic resonance ■ microvascular obstruction ■ intramyocardial hemorrhage ■ residual myocardial iron ■ ST-segment–elevation myocardial infarction ■ T2 mapping ■ T2* mapping

Although improvements in evidence-based therapies during primary percutaneous coronary intervention (PPCI) have substantially reduced mortality after an acute ST-segment–elevation myocardial infarction (STEMI), the onset of heart failure is on the rise.[1–3] Microvascular obstruction (MVO) occurs in ≈50% of reperfused STEMI patients,[4]

Received March 29, 2016; accepted August 11, 2016.

From the Hatter Cardiovascular Institute, Institute of Cardiovascular Science, University College London, United Kingdom (H.B., S.K.W., M.R., A.H., D.M.Y., D.J.H.); National Institute of Health Research, University College London Hospitals Biomedical Research Centre, United Kingdom (H.B., S.K.W., M.R., A.H., A.S., D.M.Y., J.C.M., D.J.H.); Barts Heart Centre, St Bartholomew's Hospital, London, United Kingdom (H.B., S.R., A.A.-G., S.K.W., A.N.B., T.A.T., M.F., M.R., A.H., A.S., A.S.H., C.M., J.C.M., D.J.H.); National Heart, Lung and Blood Institute, National Institutes of Health, Bethesda, MD (P.K.); Cardiovascular and Metabolic Disorders Program, Duke-National University of Singapore (D.J.H.); and National Heart Research Institute Singapore, National Heart Centre Singapore (D.J.H.).

The Data Supplement is available at http://circimaging.ahajournals.org/lookup/suppl/doi:10.1161/CIRCIMAGING.116.004940/-/DC1.

Correspondence to Derek J. Hausenloy, PhD, Cardiovascular and Metabolic Diseases Program, Duke-NUS Graduate Medical School Singapore, 8 College Rd, Singapore 169857. E-mail derek.hausenloy@duke-nus.edu.sg

and ≈40% of STEMI patients develop intramyocardial hemorrhage (IMH)[5] detected by cardiovascular magnetic resonance (CMR). Both MVO and IMH are associated with larger myocardial infarct (MI) size, adverse left ventricular (LV) remodeling, and worse clinical outcomes.[4,6–11]

See Editorial by Dharmakumar
See Clinical Perspective

LV remodeling post MI refers to the intricate changes that occur in both the infarcted and remote myocardium on a molecular, structural, geometric, and functional level,[12] and its occurrence predisposes to heart failure. The 3 partially overlapping phases during post MI LV remodeling are the inflammatory phase, the proliferative phase, and the maturation phase.[13] Numerous anti-inflammatory agents, such as glucocorticoids, monoclonal antibodies, C1 esterase inhibitors, metalloproteinase inhibitors, phosphoinositide-3-kinase inhibitors, and immunoglobulin, have had promising results in the experimental setting, but have failed to translate into the clinical setting.[14]

Therefore, new therapeutic targets are required to prevent adverse LV remodeling and to improve clinical outcomes in reperfused STEMI patients. IMH and its iron degradation products have been shown to result in residual myocardial iron within the MI zone and have been proposed to have cytotoxic and proinflammatory effects on the myocardium.[15,16] In some STEMI patients, areas of T2 abnormalities within the infarct zone have been shown to persist on CMR performed 6 months post PPCI.[17,18] The pathogenesis of the persistently elevated T2 signal and its relationship to adverse LV remodeling remains to be determined.

Therefore, we hypothesized that patients with adverse LV remodeling were more likely to (1) have MVO/IMH on the acute scan; (2) have residual myocardial iron at follow-up; and (3) have persistently elevated T2 values in surrounding areas of residual myocardial iron that may be suggestive of persistent myocardial inflammation.

Methods

Study Population

Fifty STEMI patients reperfused by PPCI were prospectively recruited between August 2013 and July 2014. The main exclusion criteria were previous MI and standard recognized contraindications to CMR, such as estimated glomerular filtration rate <30 mL/min, ferromagnetic implants, and claustrophobia. The acute CMR scan was performed at 4±2 days post STEMI and a follow-up CMR scan at 5±2 months. The UK National Research Ethics Service approved this study, and all patients provided written informed consent.

CMR Acquisition

CMR was performed on a 1.5 Tesla scanner (Magnetom Avanto; Siemens Medical Solutions) using a 32-channel phased-array cardiac coil. The imaging protocol included balanced steady-state free precession cines, native T1, T2, and T2* mapping (Work In Progress 448b; Siemens Healthcare), and late gadolinium enhancement (LGE) LV short-axis images. For the acute scan, whole LV short-axis coverage for T1 and T2 maps and 3 (basal, mid, and apical) LV short-axis slices T2* maps were acquired. On the follow-up scan, only basal, mid, and apical short-axis slices were acquired for native T1, T2, and T2* maps.

Native T1 Mapping

Native T1 maps were acquired with a steady-state free precession–based Modified Look-Locker Inversion Recovery (MOLLI) sequence using a 5s(3s)3s modified sampling protocol.[19] The acquisition parameters were flip angle =35°; pixel bandwidth =977 Hz/pixel; matrix =256×144; echo time =1.1 ms; and slice thickness =6 mm. A pixel-wise colored T1 map was generated after performing motion correction and a nonlinear least-square curve fitting of the set of images acquired at different inversion times.

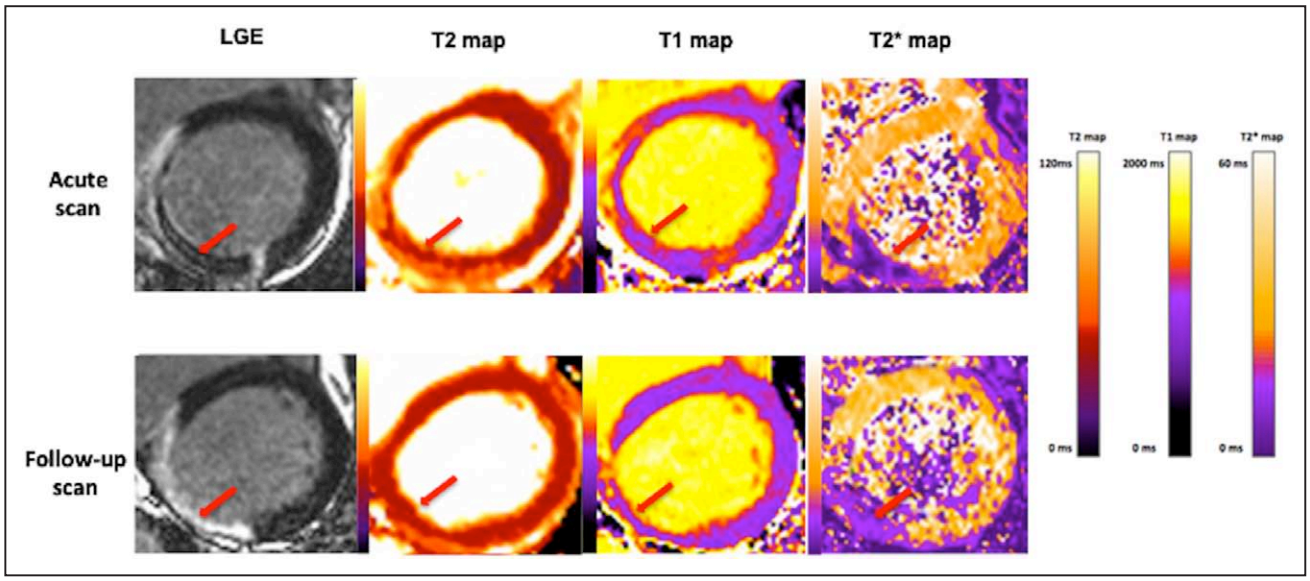

Figure 1. Basal left ventricular (LV) short axis of a patient with an acute inferior myocardial infarction (MI) depicting microvascular obstruction (MVO) on late gadolinium enhancement (LGE) scans with corresponding hypointense cores (red arrows) on the basal LV short axis T1, T2, and T2* maps and the follow-up scan with corresponding maps and areas of residual myocardial iron on the T2* map.

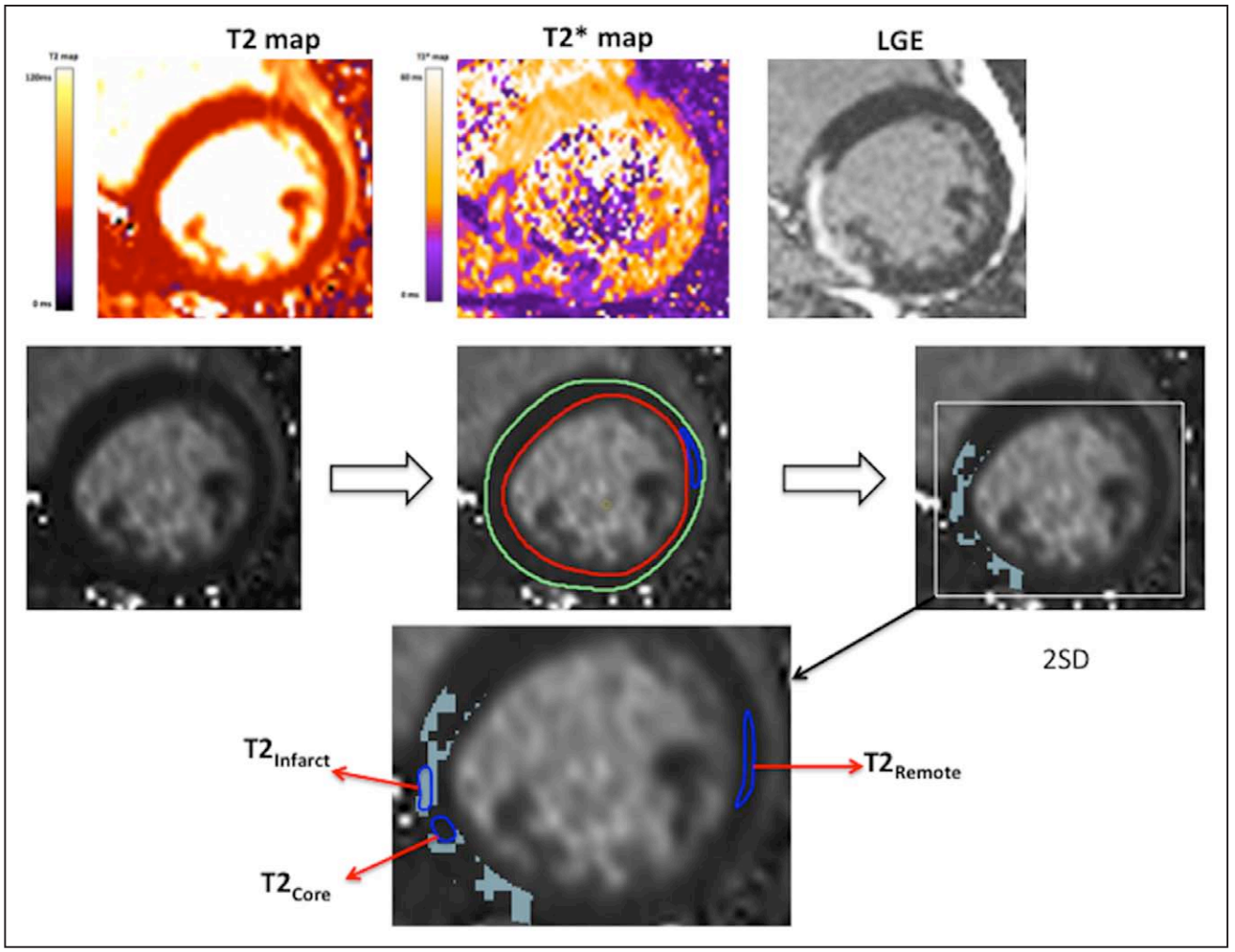

Figure 2. Method used to detect the area of high T2 ($T2_{Infarct}$) around the area of residual myocardial iron ($T2_{Core}$) and the remote myocardium ($T2_{Remote}$) using a threshold of 2 standard deviation (SD) from the remote myocardium. LGE indicates late gadolinium enhancement.

T2 Mapping

Colored T2 maps consisting of pixel-wise T2 values were generated inline after motion correction and fitting to estimate T2 relaxation times[20] after acquiring 3 single-shot images at different T2 preparation times (0, 24, and 55 ms, respectively). The acquisition parameters were flip angle =70°; pixel bandwidth =930 Hz/pixel; matrix =116×192; echo time =1.1 ms; repetition time =3×R-R interval; and slice thickness =6 mm.

T2* Mapping

T2* maps were obtained using the following imaging parameters: bandwidth 814(×8) Hz/pixel; echo times×8: 2.7, 5, 7.3, 9.6, 11.9, 14.2, 16.5, and 18.8 ms; flip angle =18°; acquisition matrix =256×115; and slice thickness =8 mm. A colored pixel-wise T2* map was generated by the scanner.

Late Gadolinium Enhancement

LGE images were acquired 10 to 15 minutes after the injection of 0.1 mmol/kg of gadoterate meglumine (Gd-DOTA marketed as Dotarem; Guerbet S.A., Paris, France), using either a standard segmented fast low-angle shot 2-dimensional inversion-recovery gradient echo sequence (n=16) or a respiratory motion-corrected, free-breathing single-shot steady-state free precession averaged phase-sensitive inversion recovery sequence[21] (n=24).

Figure 1 shows an example of the basal short axis images acquired during the acute scan and at follow-up in a patient with an inferior STEMI.

CMR Analysis

Imaging analysis was performed using CVI42 software (Version 5.1.2[303], Calgary, Canada).

Adverse LV remodeling was defined as a ≥20% increase in LV end-diastolic volume (EDV) between the acute and follow-up scans.[22]

MI size was quantified in grams and as a percentage of the LV (%LV) using a signal-intensity threshold of 5 standard deviations (SD)[23] above the mean remote myocardium. The area at risk (AAR) was assessed from the T2 maps using a signal intensity threshold of 2SD above the mean remote myocardium and expressed as %LV. The presence of MVO (late MVO) was defined as areas of hypoenhancement on the LGE images and was quantified and expressed as %LV. Areas of MVO were included as part of the MI zone and AAR.

A hypointense core on the T2* maps with a T2* value of <20 ms was used to identify the presence of IMH on the acute scans and residual myocardial iron on the follow-up scans.[24–28] The extent of IMH and residual iron was quantified using manual region of interest (ROI) delineation around the hypointense core on the basal, mid, and apical slices and expressed as %LV.

For the follow-up T1 and T2 maps, a ROI was manually drawn in hyperenhanced area using a signal intensity threshold of 2SD from the remote myocardium (using the LGE images as reference) and was denoted as $T1_{Infarct}$ and $T2_{Infarct}$, respectively.

A second ROI was copied from the hypointense core of the T2* map on to the T1 and T2 maps and denoted as $T1_{Core}$ and $T2_{Core}$ as illustrated in Figure 2.

In cases when there were no areas of hyperenhancement on the follow-up maps using a 2SD threshold, an ROI from the areas of LGE was copied on to the maps for representative values. An ROI was also drawn in the remote myocardium and expressed as $T1_{Remote}$ and $T2_{Remote}$.

Statistical Analysis

Statistical analysis was performed using SPSS version 22 (IBM Corporation, IL). Continuous data were expressed as mean±SD or median (interquartile range), and categorical data were reported as frequencies and percentages. Normality was assessed using Shapiro–Wilk test. Independent groups (those with and without IMH; with and without paired CMR scans; with and without residual iron at follow-up; with and without adverse LV remodeling; without adverse LV remodeling but with and without residual iron) were compared with unpaired Student's *t* test for normally distributed data and with Mann–Whitney *U* test for non-normally distributed data. Comparison between paired acute and follow-up scan was performed using paired Student's *t* test for normally distributed data and Wilcoxon signed-rank test for non-normally distributed data. To compare T1 and T2 values in the remote, core, and infarct territories between patients and divided between those with and without residual iron, a linear mixed model was used, with the patients as a random factor and the territory within the patients (remote, core, and infarct) being a fixed factor. Comparison of 3 independent groups (no residual iron, residual iron only, and residual iron and adverse LV remodeling) was performed using Kruskal–Wallis Test and post hoc pairwise comparisons. Categorically variables such as incidence of MVO or IMH were compared using chi-squared test or Fisher exact test. Pearson rho correlation coefficient was assessed between MVO, acute MI size, IMH, and adverse LV remodeling as a continuous variable, respectively, and their correlations were compared. Receiver operating characteristic curve was also used to compare the diagnostic performance of MVO, acute MI size, and IMH to predict adverse LV remodeling. All statistical tests were 2-tailed, and $P<0.05$ was considered statistically significant.

Results

Out of 50 STEMI patients recruited into the study, 48 STEMI patients (mean age 59±13 years old, 88% male) completed the acute scan at 4±2 days post PPCI, and 40 of these patients had a follow-up scan at 5±2 months. Two patients did not complete the scans because of unexpected claustrophobia. Characteristics of the 40 patients with a follow-up scan included in this study are listed in Table 1. CMR details of these 40 patients are shown in Table 2. A CONSORT (Consolidated Standards of Reporting Trials) flow diagram is provided in the Data Supplement. The median chest pain onset to PPCI time was 267 (122–330) minutes. No patients had heart failure at baseline. The MI size was 27.4±14.6 %LV, and T2-based AAR was 42.7±11.9 %LV. MVO was present in 65% (26/40) of patients (mean MVO size of 13.6±7.2 %LV). In 24% of scans, the T2* maps (acute and follow-up) had to be excluded because they were not interpretable because of motion and off-resonance artifacts. After a mean follow-up of 5±2 months, 2 patients were rehospitalized for heart failure, and there were no deaths.

IMH and Edema-Based AAR

Patients with IMH had lower $T2_{Core}$ (50 [46–53] ms versus 55 [52-59] ms; $P=0.001$) but similar $T2_{Infarct}$ (64 [62–64] ms versus 64 [62–69] ms; $P=0.29$) and T2 in the salvaged myocardium (65 [61–68] ms versus 63 [62–67] ms; $P=0.43$). However, in patients with IMH, edema-based AAR was larger (46 [40–55] %LV versus 31 [24–43] %LV; $P=0.009$) and

Table 1. Clinical Characteristics of STEMI Patients

Details	Number
Number of patients	40
Male (%)	35 (88%)
Age (years)	59±13
Diabetes mellitus	8 (20%)
Hypertension	14 (35%)
Smoking	12 (30%)
Dyslipidemia	14 (35%)
Heart failure at baseline	0
Chest pain onset to PPCI time (minutes)	267 (122–330)
Infarct artery (%)	
LAD	24 (60%)
RCA	14 (35%)
Cx	2 (5%)
Treatment: on discharge	
Dual antiplatelet therapy	40 (100%)
Beta blockers	40 (100%)
ACEI/ARB	40 (100%)
Statin	39 (98%)
MRA	10 (25%)

ACEI/ARB indicates angiotensin-converting enzyme inhibitor/angiotensin receptor blocker; Cx, circumflex artery; LAD, left anterior descending artery; MRA, mineralocorticoid receptor antagonist; PPCI, primary percutaneous coronary intervention; RCA, right coronary artery; STEMI, ST-segment–elevation myocardial infarction; TIMI, Thrombolysis in Myocardial Infarction.

Table 2. CMR Characteristics of STEMI Patients

	Acute Scan (n=40)	Follow-Up Scan (n=40)	*P* Value
EDV, mL	172±38	182±49	0.027
ESV, mL	90±30	88±38	0.60
EF, %	49±8	53±10	0.001
LV mass, g	112±35	104±26	0.051
Infarct size, % of LV	27.4±14.6	19.5±10.5	0.0001
Infarct size, g	20.2±13.6	14.4±9.4	0.0001
T2-based AAR, % of LV	42.0±12%	…	NA
MVO, n (%)	26 (65)	…	NA
MVO (n=26), %LV	5.1±3.5		NA
IMH (n=15), %LV	14.0 (6.0–21.2)	…	NA
Residual iron (n=13), %LV	…	9.0 (4.0–10.3)	NA
$T2_{Remote}$, ms			
T2*<20 ms (n=15)	51 (48–53)	49 (46–51)	0.056
T2*≥20 ms (n=13)	49 (48–51)	47 (45–48)	0.060
$T2_{Infarct}$, ms			
T2*<20 ms (n=15)	64 (62–68)	60 (58–64)	0.017
T2*≥20 ms (n=13)	64 (62–69)	53 (51–55)	0.001
$T2_{Core}$, ms			
T2*<20 ms (n=15)	50 (46–53)	47 (45–50)	0.111
T2*≥20 ms (n=13)	55 (52–59)	47 (45–49)	0.001
$T1_{Remote}$, ms			
T2*<20 ms (n=15)	1051 (1023–1094)	1015 (989–1020)	0.002
T2*≥20 ms (n=13)	990 (968–1018)	1007 (966–1039)	0.74
$T1_{Infarct}$, ms			
T2*<20 ms (n=15)	1232 (1163–1338)	1162 (1132–1216)	0.014
T2*≥20 ms (n=13)	1262 (1198–1286)	1113 (1092–1140)	0.001
$T1_{Core}$, ms			
T2*<20 ms (n=15)	1016 (949–1061)	1004 (990–1028)	0.78
T2*≥20 ms (n=13)	1140 (1086–1160)	1042 (1015–1140)	0.11
$T2^*_{Remote}$ (n=28)	32 (30–35)	34 (31–35)	0.52
$T2^*_{Infarct}$ (n=13)	29 (24–36)	33 (28–35)	0.80
$T2^*_{Core}$ (n=15)	10 (11–13)	15 (13–17)	0.013

AAR indicates area at risk; CMR, cardiovascular magnetic resonance; EDV, end-diastolic volume; EF, ejection fraction; ESV, end-systolic volume; IMH, intramyocardial hemorrhage; LV, left ventricle; MVO, microvascular obstruction; NA, not applicable; STEMI, ST-segment–elevation myocardial infarction.

myocardial salvage index was smaller (0.24 [0.16–0.43] versus 0.61 [0.36–0.88]; *P*=0.009), when compared with those without IMH.

Residual Myocardial Iron on the Follow-Up Scan in a Subset of Patients

A subset of 28 patients who completed the follow-up scans had matching and interpretable T2* maps. There was no difference in the CMR parameters between those with paired T2* maps (n=28) and those without (n=12; see Table in the Data Supplement). On the acute scan, 15/28 (54%) patients had IMH and 18/28 (64%) had MVO. Fifteen of 18 (83%) patients had MVO with IMH. On the follow-up scan, 13/15 (87%) patients had evidence of residual myocardial iron.

T1 and T2 of the Core, Infarct Zone, and Remote Myocardium at Follow-Up

Using a linear mixed model to adjust for within-patient interaction, in patients without residual myocardial iron, there was no difference between $T1_{Core}$ and $T1_{Infarct}$ (1042 [1015–1140] ms versus 1113 [1092–1140] ms; *P*=0.20), and $T1_{Infarct}$ was significantly higher than $T1_{Remote}$ (1113

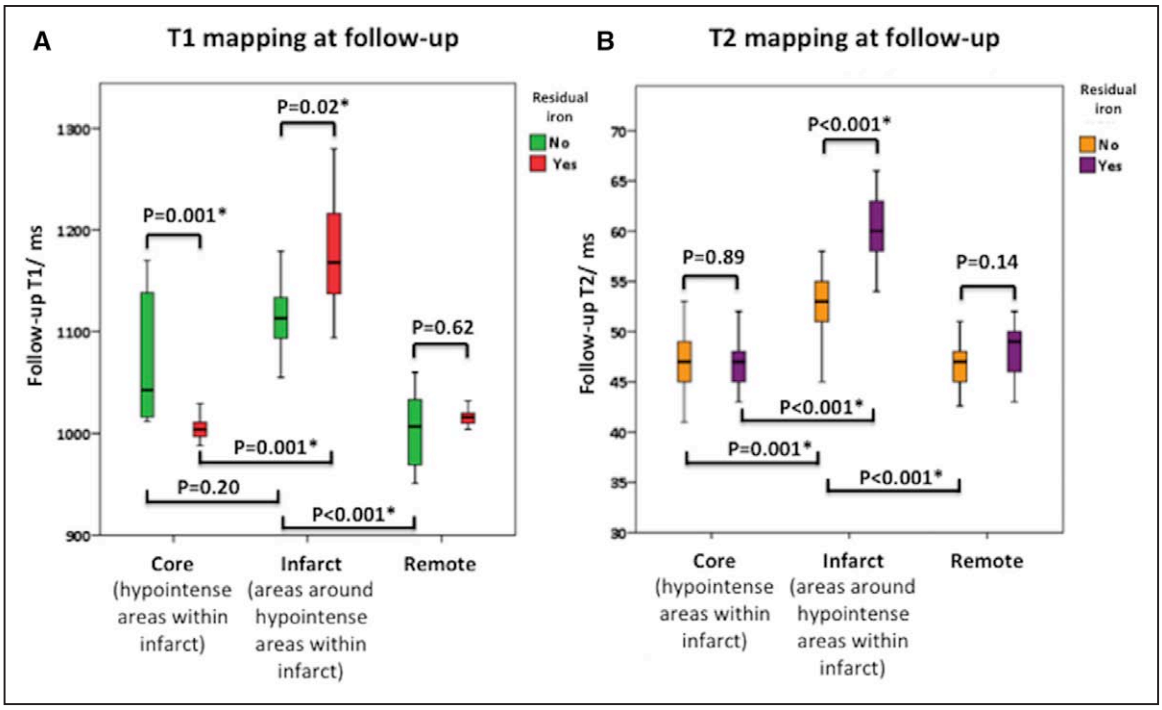

Figure 3. Box plots of T1 (**A**) and T2 (**B**) values of the core, infarct, and remote myocardium in patients with and without residual myocardial iron.

[1092–1140] ms versus 1007 [966–1039] ms; $P<0.001$). However, $T2_{Core}$ was lower than $T2_{Infarct}$ (47 [45–49] ms versus 53 [51–55] ms; $P=0.001$) and similar to $T2_{Remote}$ (47 [45–49] ms versus 47 [45–48] ms; $P=1.0$), and $T2_{Infarct}$ was significantly higher than $T2_{Remote}$ (53 [51–55] ms versus 47 [45–48] ms; $P<0.001$; Figure 3).

In patients with residual myocardial iron, both $T1_{Core}$ and $T2_{Core}$ were similar to $T1_{Remote}$ and $T2_{Remote}$ (T1: 1004 [90–1028] ms versus 1015 [989–1020] ms; $P=1.0$; T2: 47 [45–50] ms versus 49 [46–51] ms; $P=1.0$) but significantly lower than $T1_{Infarct}$ and $T2_{Infarct}$ (T1: 1004 [90–1028] ms versus 1162 [1132–1216] ms; $P<0.001$; T2: 47 [45–50] ms versus 60 [58–64] ms; $P<0.001$) respectively (Figure 3).

Patients with residual myocardial iron had lower $T1_{Core}$, similar $T2_{Core}$, and higher $T1_{Infarct}$ and $T2_{Infarct}$ when compared with patients without. There was no difference in the $T1_{Remote}$ and $T2_{Remote}$ between these 2 groups as illustrated in Figure 3.

Figure 4 shows an example of 3 patients with acute and follow-up CMR images showing MVO, IMH, residual myocardial iron, and persistently elevated T2 in the surrounding myocardium within the infarct zone at follow-up.

IMH and Adverse LV Remodeling

Eight out of 40 (20%) patients developed adverse LV remodeling. Patients with adverse LV remodeling had larger MI size (30.1±7.3 %LV versus 16.9±9.8 %LV; $P=0.01$), had an increased incidence (100% versus 50%; $P=0.10$) and extent of MVO (8.0±3.2 %LV versus 3.6±2.6 %LV; $P=0.001$), and were more likely to have IMH (100% versus 60%; $P=0.04$) on the acute scans when compared with those without adverse LV remodeling.

Residual Myocardial Iron and Adverse LV Remodeling

In patients with adverse LV remodeling, $T2_{Infarct}$ was significantly higher than in those without adverse LV remodeling and without residual myocardial iron (60 [54–64] ms versus 53 [51–56] ms; $P=0.025$), but similar to those with residual myocardial iron but no adverse LV remodeling (60 [54–64] ms versus 60 [58–63] ms; $P=1.0$) as shown in Figure 5A.

However, when looking at those patients who did not develop adverse LV remodeling, those with residual iron had a significantly higher change in EDV (8% [−2% to 14%] versus −4% [−7% to 5%]; $P=0.043$) when compared with those patients without residual myocardial iron (Figure 5B).

Relationship Between Acute MI Size, MVO, and IMH and Adverse LV Remodeling

Acute MI size, extent of MVO, and IMH correlated with the change in LV EDV (Pearson's rho of 0.64, 0.59, and 0.66, respectively; P values of 0.18 and 0.62, respectively, for correlation coefficient comparison) and performed equally well on receiver operating characteristic curve for predicting adverse LV remodeling (area under the curve: 0.99, 0.94, and 0.95, respectively, $P=0.19$ for receiver operating characteristic curve comparison).

Discussion

The major findings of our study are as follows: (1) the majority of STEMI patients treated by PPCI with MVO also had IMH (83%); (2) many of these patients with IMH had residual myocardial iron at follow-up (87%), and these patients had elevated T2 values on CMR in the surrounding myocardium in the MI zone, suggestive of delayed

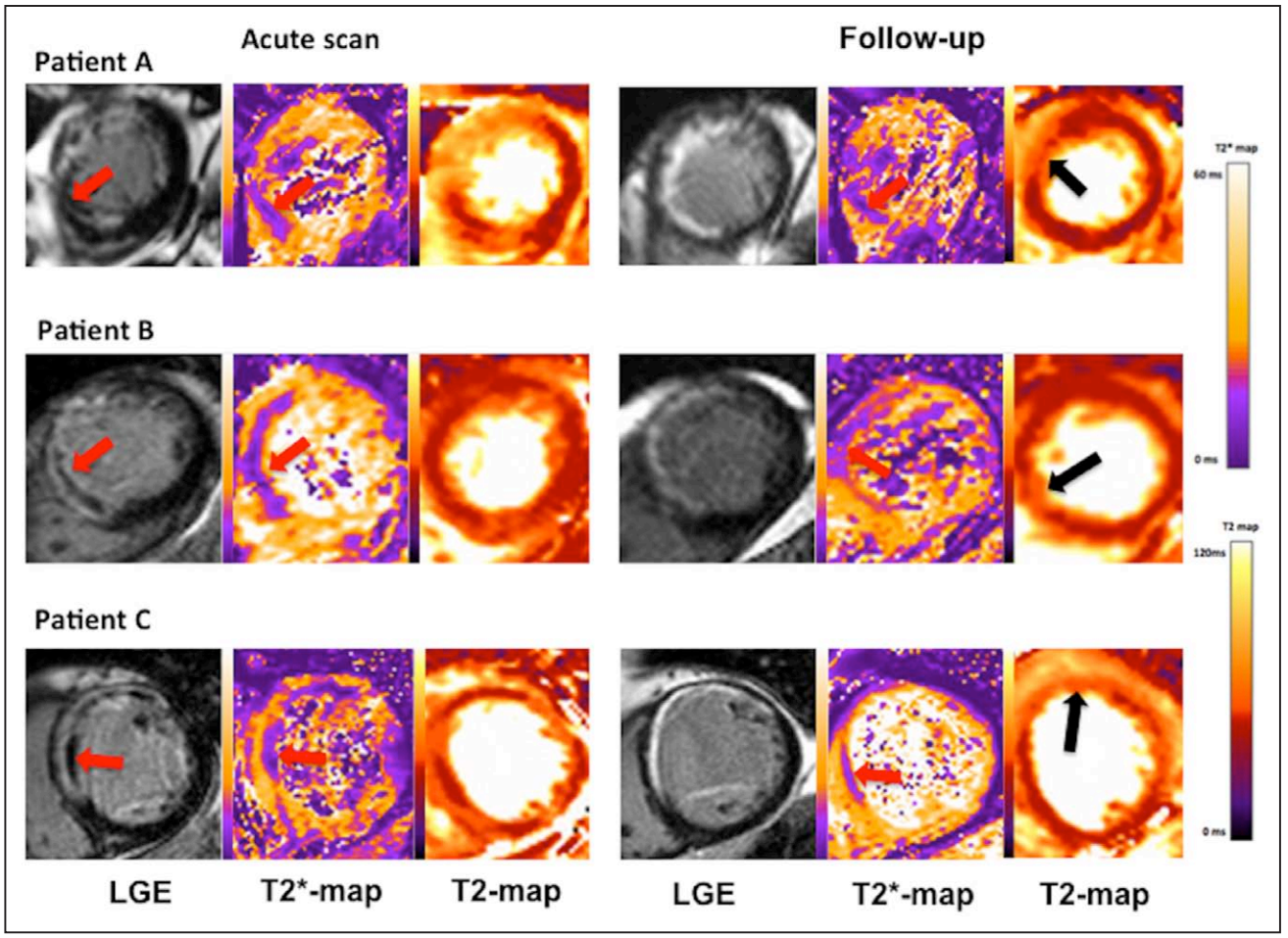

Figure 4. Examples of 3 patients (**A**, **B**, and **C**) with acute and follow-up scans and the red arrows showing areas of microvascular obstruction (MVO), intramyocardial hemorrhage (IMH), and residual myocardial iron and the black arrows showing areas of hyperenhancement on the T2 maps. LGE indicates late gadolinium enhancement.

resolution of edema or inflammation; (3) all patients with adverse LV remodeling had residual myocardial iron and elevated T2 in the surrounding myocardium in the MI zone; and (4) acute MI size, the extent of MVO, and IMH correlated equally well with the change in LV EDV and performed with high diagnostic accuracy to predict adverse LV remodeling.

Furthermore, in patients not meeting the definition for adverse LV remodeling, those with residual myocardial iron had a larger percentage increase in EDV than those without residual myocardial iron, confirming an overlap between the inflammatory phase and proliferation phase previously described.[13] Although T1 values were also higher in the MI zone surrounding areas of residual myocardial iron compared with those without, this difference in T1 may have been because of the complex interplay between fibrosis, edema, and the development of early fatty metaplasia[29] in the chronic phase of a STEMI.

It is well recognized that IMH is associated with larger MI size, adverse LV remodeling, and poor clinical outcomes[6,9,30,31] and may be proarrhythmic.[32,33] Although our study was purely based on tissue characterization, these findings support the current literature that residual myocardial iron may play a role in the inflammatory phase of adverse LV remodeling. Using T2* imaging, Kali et al[15] have recently shown in a small cohort of 15 STEMI patients that the presence of IMH on the acute CMR scans was associated with residual myocardial iron at 6 months. They also used immunohistochemical analysis of canine hearts subjected to acute MI to show evidence of localized accumulation of macrophages at the sites of chronic iron deposition at follow-up, suggesting a prolonged inflammatory response at the sites of residual myocardial iron.[15] Roghi et al[16] also showed in a small cohort of 15 STEMI patients that those with MVO and IMH had higher levels of nontransferrin-bound iron—these have previously been linked to cardiotoxicity in thalassemia major. Our study is the first study to use T2 mapping for the detection of delayed resolution of edema associated with residual myocardial iron in patients with IMH.

Recently, Carrick et al[34] performed serial scanning in 30 patients and elegantly described the time course of MVO and IMH. MVO was already present at 4 to 12 hours and remained stable up to a mean of 2.9 days and then reduced by day 10. IMH, on the contrary, peaked at a mean of 2.9 days and decreased by day 10. Of note, 13 patients had IMH on day 2.9, and only 4 patients displayed residual myocardial iron by 6 months. Based on brain imaging data,[35] degradation of hemoglobin eventually leads to ferritin and hemosiderin deposits, and the fact that the majority of their patients had no residual

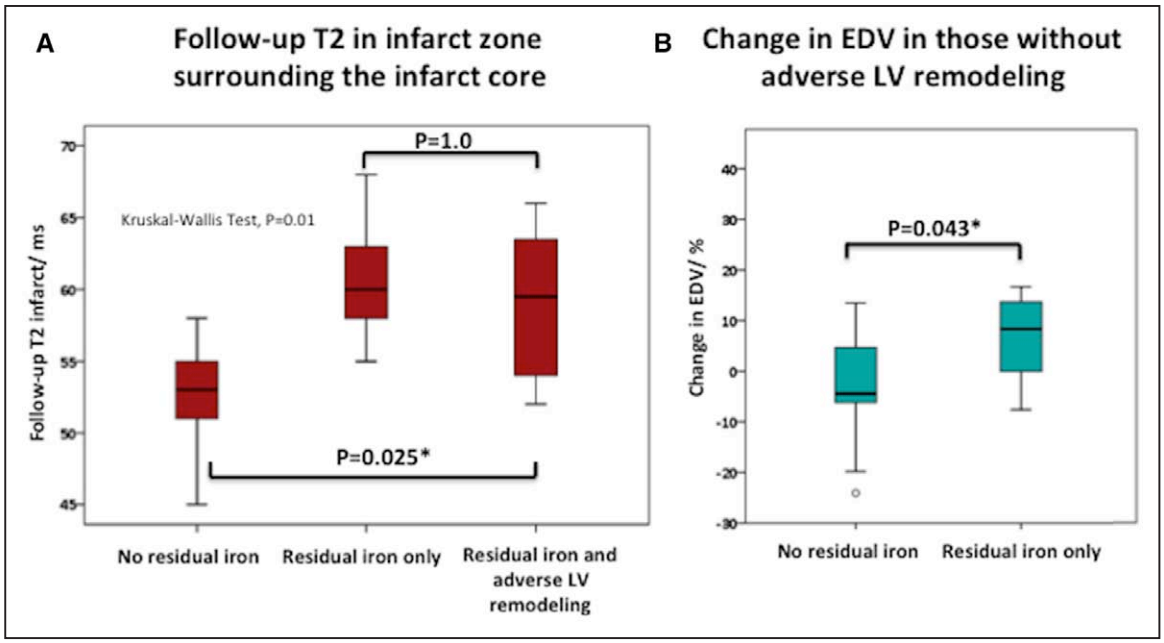

Figure 5. **A**, T2 values in the infarct zone in patients with and without residual myocardial iron. **B**, Change in end-diastolic volume (EDV) in patients without adverse left ventricular (LV) remodeling and with or without residual myocardial iron.

myocardial iron in their study may suggest that those patients had small areas of IMH that were rapidly cleared by the macrophages. They reported the presence of IMH in 41% of their total cohort of 245 patients with analyzable T2* data, and it is likely that they may have underestimated the true prevalence of IMH because the CMR was performed at a mean of 2.1 days and some patients who would have subsequently developed IMH up to 3 days post reperfusion may not have been detected.

Pooling the results of these 3 studies demonstrating residual myocardial iron after STEMI, Kali et al[15] (acute scan: 11 out of 15 patients with IMH; follow-up scan: 11 with residual myocardial iron), Carrick et al[34] (acute scan: 13 out of 30 patients with IMH; follow-up scan: 4 with residual myocardial iron), and our study (acute scan: 15 out of 28 patients with IMH; follow-up scan: 13 with residual myocardial iron), the prevalence of IMH by T2* mapping was 53% (39/73), and 72% (28/39) had residual myocardial iron at follow-up. Although IMH is likely to be confounded by larger infarct size, whether specifically targeting these patients with anti-inflammatory agents or chelation therapy needs to be investigated in further studies aiming to prevent adverse LV remodeling.

Limitations

A significant proportion of the T2* maps were not interpretable in our study, and this partly highlights the challenge of performing a comprehensive CMR scan with multiparametric mapping in patients with an acute STEMI and may be partly because of the suboptimal per-slice rather than whole-heart shimming protocol we used. Of note, 18% of T2* data were not available in the large study by Carrick et al[34] either because of patients' intolerance of the scan or non-interpretable T2* maps. Although we quantified the extent of IMH in our study, we only used basal, mid, and apical short-axis T2* maps, and the quantification may have been more accurate if whole LV coverage T2* maps had been performed. Furthermore, only basal, mid, and apical short-axis T1 and T2 maps were acquired at follow-up. We used 2 different LGE sequences, and the difference in signal-to-noise ratio between the 2 may have affected the MVO size quantification. LGE images were acquired between 10 and 15 minutes, and this may have overestimated the MI and MVO size, and whether acquiring LGE images at 25 minutes[36] would have yielded different diagnostic performances for LGE, MVO, and IMH to predict adverse LV remodeling warrants further investigation. Receiver operating characteristic curve analysis was performed in 28 patients only, and therefore, we did not provide data on sensitivity/specificity and cutoff values because of small sample size. We did not measure blood inflammation markers to support the proposal of persistent inflammation because of residual myocardial iron in these patients. Histological validation is required to determine whether the elevated T2 values in the myocardium surrounding residual iron in the infarct zone was because of persistent inflammation. Our study was small, and we could not establish a causal relationship between IMH and adverse LV remodeling.

Conclusion

The majority of reperfused STEMI patients with IMH had residual myocardial iron at follow-up. This was associated with adverse LV remodeling and persistently elevated T2 values in the surrounding infarct tissue and may be suggestive of ongoing inflammation. Furthermore, IMH was as strongly associated with adverse LV remodeling as acute MI size and MVO. Therefore, patients with IMH or residual myocardial iron could be future potential targets for therapeutic interventions with anti-inflammatory agents or chelation therapy aiming to prevent adverse LV remodeling and improve clinical outcomes in these patients.

Acknowledgments

We express our gratitude to the staff and patients at the UCLH Heart Hospital and Peter Weale for providing us with the Work In Progress investigational sequences under a research collaboration agreement with Siemens Healthcare.

Sources of Funding

This work was supported by the British Heart Foundation (FS/10/039/28270), the Rosetrees Trust, and the National Institute for Health Research University College London Hospitals Biomedical Research Centre.

Disclosures

None.

References

1. Torabi A, Cleland JG, Khan NK, Loh PH, Clark AL, Alamgir F, Caplin JL, Rigby AS, Goode K. The timing of development and subsequent clinical course of heart failure after a myocardial infarction. *Eur Heart J*. 2008;29:859–870. doi: 10.1093/eurheartj/ehn096.
2. Ezekowitz JA, Kaul P, Bakal JA, Armstrong PW, Welsh RC, McAlister FA. Declining in-hospital mortality and increasing heart failure incidence in elderly patients with first myocardial infarction. *J Am Coll Cardiol*. 2009;53:13–20. doi: 10.1016/j.jacc.2008.08.067.
3. Levi F, Lucchini F, Negri E, La Vecchia C. Trends in mortality from cardiovascular and cerebrovascular diseases in Europe and other areas of the world. *Heart*. 2002;88:119–124.
4. van Kranenburg M, Magro M, Thiele H, de Waha S, Eitel I, Cochet A, Cottin Y, Atar D, Buser P, Wu E, Lee D, Bodi V, Klug G, Metzler B, Delewi R, Bernhardt P, Rottbauer W, Boersma E, Zijlstra F, van Geuns RJ. Prognostic value of microvascular obstruction and infarct size, as measured by CMR in STEMI patients. *JACC Cardiovasc Imaging*. 2014;7:930–939. doi: 10.1016/j.jcmg.2014.05.010.
5. Carrick D, Haig C, Ahmed N, Eteiba H, McEntegart M, Watkins S, Lindsay M, Radjenovic A, Oldroyd KG, Berry C. Myocardial haemorrhage after acute reperfused ST-elevation myocardial infarction: temporal evolution, relation to microvascular obstruction and prognostic significance. *Heart*. 2015;101:A4–A5. doi: 10.1136/heartjnl-2015-307845.8.
6. Ganame J, Messalli G, Dymarkowski S, Rademakers FE, Desmet W, Van de Werf F, Bogaert J. Impact of myocardial haemorrhage on left ventricular function and remodelling in patients with reperfused acute myocardial infarction. *Eur Heart J*. 2009;30:1440–1449. doi: 10.1093/eurheartj/ehp093.
7. Ørn S, Manhenke C, Greve OJ, Larsen AI, Bonarjee VV, Edvardsen T, Dickstein K. Microvascular obstruction is a major determinant of infarct healing and subsequent left ventricular remodelling following primary percutaneous coronary intervention. *Eur Heart J*. 2009;30:1978–1985. doi: 10.1093/eurheartj/ehp219.
8. Beek AM, Nijveldt R, van Rossum AC. Intramyocardial hemorrhage and microvascular obstruction after primary percutaneous coronary intervention. *Int J Cardiovasc Imaging*. 2010;26:49–55.
9. Eitel I, Kubusch K, Strohm O, Desch S, Mikami Y, de Waha S, Gutberlet M, Schuler G, Friedrich MG, Thiele H. Prognostic value and determinants of a hypointense infarct core in T2-weighted cardiac magnetic resonance in acute reperfused ST-elevation-myocardial infarction. *Circ Cardiovasc Imaging*. 2011;4:354–362. doi: 10.1161/CIRCIMAGING.110.960500.
10. de Waha S, Desch S, Eitel I, Fuernau G, Lurz P, Leuschner A, Grothoff M, Gutberlet M, Schuler G, Thiele H. Relationship and prognostic value of microvascular obstruction and infarct size in ST-elevation myocardial infarction as visualized by magnetic resonance imaging. *Clin Res Cardiol*. 2012;101:487–495. doi: 10.1007/s00392-012-0419-3.
11. Hamirani YS, Wong A, Kramer CM, Salerno M. Effect of microvascular obstruction and intramyocardial hemorrhage by CMR on LV remodeling and outcomes after myocardial infarction: a systematic review and meta-analysis. *JACC Cardiovasc Imaging*. 2014;7:940–952. doi: 10.1016/j.jcmg.2014.06.012.
12. Pfeffer JM, Pfeffer MA, Braunwald E. Influence of chronic captopril therapy on the infarcted left ventricle of the rat. *Circ Res*. 1985;57:84–95.
13. Frangogiannis NG. The immune system and the remodeling infarcted heart: cell biological insights and therapeutic opportunities. *J Cardiovasc Pharmacol*. 2014;63:185–195. doi: 10.1097/FJC.0000000000000003.
14. Seropian IM, Toldo S, Van Tassell BW, Abbate A. Anti-inflammatory strategies for ventricular remodeling following ST-segment elevation acute myocardial infarction. *J Am Coll Cardiol*. 2014;63:1593–1603. doi: 10.1016/j.jacc.2014.01.014.
15. Kali A, Kumar A, Cokic I, Tang RL, Tsaftaris SA, Friedrich MG, Dharmakumar R. Chronic manifestation of postreperfusion intramyocardial hemorrhage as regional iron deposition: a cardiovascular magnetic resonance study with ex vivo validation. *Circ Cardiovasc Imaging*. 2013;6:218–228. doi: 10.1161/CIRCIMAGING.112.000133.
16. Roghi A, Poggiali E, Duca L, Mafrici A, Pedrotti P, Paccagnini S, Brenna S, Galli A, Consonni D, Cappellini MD. Role of non-transferrin-bound iron in the pathogenesis of cardiotoxicity in patients with ST-elevation myocardial infarction assessed by cardiac magnetic resonance imaging. *Int J Cardiol*. 2015;199:326–332. doi: 10.1016/j.ijcard.2015.07.056.
17. Carlsson M, Ubachs JF, Hedström E, Heiberg E, Jovinge S, Arheden H. Myocardium at risk after acute infarction in humans on cardiac magnetic resonance: quantitative assessment during follow-up and validation with single-photon emission computed tomography. *JACC Cardiovasc Imaging*. 2009;2:569–576. doi: 10.1016/j.jcmg.2008.11.018.
18. Dall'Armellina E, Karia N, Lindsay AC, Karamitsos TD, Ferreira V, Robson MD, Kellman P, Francis JM, Forfar C, Prendergast BD, Banning AP, Channon KM, Kharbanda RK, Neubauer S, Choudhury RP. Dynamic changes of edema and late gadolinium enhancement after acute myocardial infarction and their relationship to functional recovery and salvage index. *Circ Cardiovasc Imaging*. 2011;4:228–236. doi: 10.1161/CIRCIMAGING.111.963421.
19. Kellman P, Hansen MS. T1-mapping in the heart: accuracy and precision. *J Cardiovasc Magn Reson*. 2014;16:2. doi: 10.1186/1532-429X-16-2.
20. Giri S, Chung YC, Merchant A, Mihai G, Rajagopalan S, Raman SV, Simonetti OP. T2 quantification for improved detection of myocardial edema. *J Cardiovasc Magn Reson*. 2009;11:56. doi: 10.1186/1532-429X-11-56.
21. Kellman P, Arai AE. Cardiac imaging techniques for physicians: late enhancement. *J Magn Reson Imaging*. 2012;36:529–542. doi: 10.1002/jmri.23605.
22. Carrick D, Haig C, Rauhalammi S, Ahmed N, Mordi I, McEntegart M, Petrie MC, Eteiba H, Lindsay M, Watkins S, Hood S, Davie A, Mahrous A, Sattar N, Welsh P, Tzemos N, Radjenovic A, Ford I, Oldroyd KG, Berry C. Pathophysiology of LV remodeling in survivors of STEMI: inflammation, remote myocardium, and prognosis. *J AM COLL CARDIOL. Cardiovasc Imaging*. 2015;8:779–789. doi: 10.1016/j.jcmg.2015.03.007.
23. Schulz-Menger J, Bluemke DA, Bremerich J, Flamm SD, Fogel MA, Friedrich MG, Kim RJ, von Knobelsdorff-Brenkenhoff F, Kramer CM, Pennell DJ, Plein S, Nagel E. Standardized image interpretation and post processing in cardiovascular magnetic resonance: Society for Cardiovascular Magnetic Resonance (SCMR) board of trustees task force on standardized post processing. *J Cardiovasc Magn Reson*. 2013;15:35. doi: 10.1186/1532-429X-15-35.
24. Kandler D, Lücke C, Grothoff M, Andres C, Lehmkuhl L, Nitzsche S, Riese F, Mende M, de Waha S, Desch S, Lurz P, Eitel I, Gutberlet M. The relation between hypointense core, microvascular obstruction and intramyocardial haemorrhage in acute reperfused myocardial infarction assessed by cardiac magnetic resonance imaging. *Eur Radiol*. 2014;24:3277–3288. doi: 10.1007/s00330-014-3318-3.
25. O'Regan DP, Ariff B, Neuwirth C, Tan Y, Durighel G, Cook SA. Assessment of severe reperfusion injury with T2* cardiac MRI in patients with acute myocardial infarction. *Heart*. 2010;96:1885–1891. doi: 10.1136/hrt.2010.200634.
26. Kidambi A, Mather AN, Motwani M, Swoboda P, Uddin A, Greenwood JP, Plein S. The effect of microvascular obstruction and intramyocardial hemorrhage on contractile recovery in reperfused myocardial infarction: insights from cardiovascular magnetic resonance. *J Cardiovasc Magn Reson*. 2013;15:58. doi: 10.1186/1532-429X-15-58.
27. Kali A, Tang RL, Kumar A, Min JK, Dharmakumar R. Detection of acute reperfusion myocardial hemorrhage with cardiac MR imaging: T2 versus T2. *Radiology*. 2013;269:387–395. doi: 10.1148/radiol.13122397.
28. Carrick D, Haig C, Rauhalammi S, Ahmed N, Mordi I, McEntegart M, Petrie MC, Eteiba H, Hood S, Watkins S, Lindsay M, Mahrous A, Ford I, Tzemos N, Sattar N, Welsh P, Radjenovic A, Oldroyd KG, Berry C. Prognostic significance of infarct core pathology revealed by quantitative non-contrast in comparison with contrast cardiac magnetic resonance imaging in reperfused ST-elevation myocardial infarction survivors. *Eur Heart J*. 2016;37:1044–1059. doi: 10.1093/eurheartj/ehv372.
29. Kellman P, Bandettini WP, Mancini C, Hammer-Hansen S, Hansen MS, Arai AE. Characterization of myocardial T1-mapping bias caused by intramyocardial fat in inversion recovery and saturation recovery techniques. *J Cardiovasc Magn Reson*. 2015;17:33. doi: 10.1186/s12968-015-0136-y.

30. Bekkers SC, Smulders MW, Passos VL, Leiner T, Waltenberger J, Gorgels AP, Schalla S. Clinical implications of microvascular obstruction and intramyocardial haemorrhage in acute myocardial infarction using cardiovascular magnetic resonance imaging. *Eur Radiol*. 2010;20:2572–2578. doi: 10.1007/s00330-010-1849-9.
31. Mather AN, Fairbairn TA, Ball SG, Greenwood JP, Plein S. Reperfusion haemorrhage as determined by cardiovascular MRI is a predictor of adverse left ventricular remodelling and markers of late arrhythmic risk. *Heart*. 2011;97:453–459. doi: 10.1136/hrt.2010.202028.
32. Cokic I, Kali A, Wang X, Yang HJ, Tang RL, Thajudeen A, Shehata M, Amorn AM, Liu E, Stewart B, Bennett N, Harlev D, Tsaftaris SA, Jackman WM, Chugh SS, Dharmakumar R. Iron deposition following chronic myocardial infarction as a substrate for cardiac electrical anomalies: initial findings in a canine model. *PLoS One*. 2013;8:e73193. doi: 10.1371/journal.pone.0073193.
33. Cokic I, Kali A, Yang HJ, Yee R, Tang R, Tighiouart M, Wang X, Jackman WS, Chugh SS, White JA, Dharmakumar R. Iron-sensitive cardiac magnetic resonance imaging for prediction of ventricular arrhythmia risk in patients with chronic myocardial infarction: early evidence. *Circ Cardiovasc Imaging*. 2015;8:e003642. doi: 10.1161/CIRCIMAGING.115.003642.
34. Carrick D, Haig C, Ahmed N, McEntegart M, Petrie MC, Eteiba H, Hood S, Watkins S, Lindsay MM, Davie A, Mahrous A, Mordi I, Rauhalammi S, Sattar N, Welsh P, Radjenovic A, Ford I, Oldroyd KG, Berry C. Myocardial hemorrhage after acute reperfused ST-segment-elevation myocardial infarction: relation to microvascular obstruction and prognostic significance. *Circ Cardiovasc Imaging*. 2016;9:e004148. doi: 10.1161/CIRCIMAGING.115.004148.
35. Bradley WG Jr. MR appearance of hemorrhage in the brain. *Radiology*. 1993;189:15–26. doi: 10.1148/radiology.189.1.8372185.
36. Rodríguez-Palomares JF, Ortiz-Pérez JT, Lee DC, Bucciarelli-Ducci C, Tejedor P, Bonow RO, Wu E. Time elapsed after contrast injection is crucial to determine infarct transmurality and myocardial functional recovery after an acute myocardial infarction. *J Cardiovasc Magn Reson*. 2015;17:43. doi: 10.1186/s12968-015-0139-8.

CLINICAL PERSPECTIVE

It is already known that ≈50% of ST-segment–elevation myocardial infarction patients develop microvascular obstruction, despite prompt reperfusion of the epicardial vessel by primary percutaneous coronary intervention, and this is associated with adverse left ventricular remodeling and worse clinical outcomes. However, the impact of intramyocardial hemorrhage on the same end points has not been clearly established. Our study analyzed paired cardiovascular magnetic resonance scans in 40 ST-segment–elevation myocardial infarction patients within 1 week and at 5 months after primary percutaneous coronary intervention. Twenty-eight patients also had paired T2* mapping data available. We found that the large majority (83%) of the patients with microvascular obstruction also had intramyocardial hemorrhage. Many of these patients went on to have residual myocardial iron at follow-up (87%) as identified by T2* mapping, and this was associated with persistently elevated T2 values in the surrounding infarct tissue. Furthermore, intramyocardial hemorrhage was as strongly associated with adverse left ventricular remodeling as acute myocardial infarction size and microvascular obstruction. These findings suggest that intramyocardial hemorrhage and residual iron within the infarct zone may be associated with delayed resolution of edema or inflammation and adverse left ventricular remodeling. Therefore, whether anti-inflammatory agents or iron chelation therapy may prevent adverse left ventricular remodeling and improve clinical outcomes in ST-segment–elevation myocardial infarction patients treated by primary percutaneous coronary intervention warrants further investigation.

Residual Myocardial Iron Following Intramyocardial Hemorrhage During the Convalescent Phase of Reperfused ST-Segment–Elevation Myocardial Infarction and Adverse Left Ventricular Remodeling

Heerajnarain Bulluck, Stefania Rosmini, Amna Abdel-Gadir, Steven K. White, Anish N. Bhuva, Thomas A. Treibel, Marianna Fontana, Manish Ramlall, Ashraf Hamarneh, Alex Sirker, Anna S. Herrey, Charlotte Manisty, Derek M. Yellon, Peter Kellman, James C. Moon and Derek J. Hausenloy

Circ Cardiovasc Imaging. 2016;9:
doi: 10.1161/CIRCIMAGING.116.004940
Circulation: Cardiovascular Imaging is published by the American Heart Association, 7272 Greenville Avenue, Dallas, TX 75231

Print ISSN: 1941-9651. Online ISSN: 1942-0080

Supplemental Material

CONSORT flow diagram: illustration of number of patients recruited and scanned at the 2 time-points.

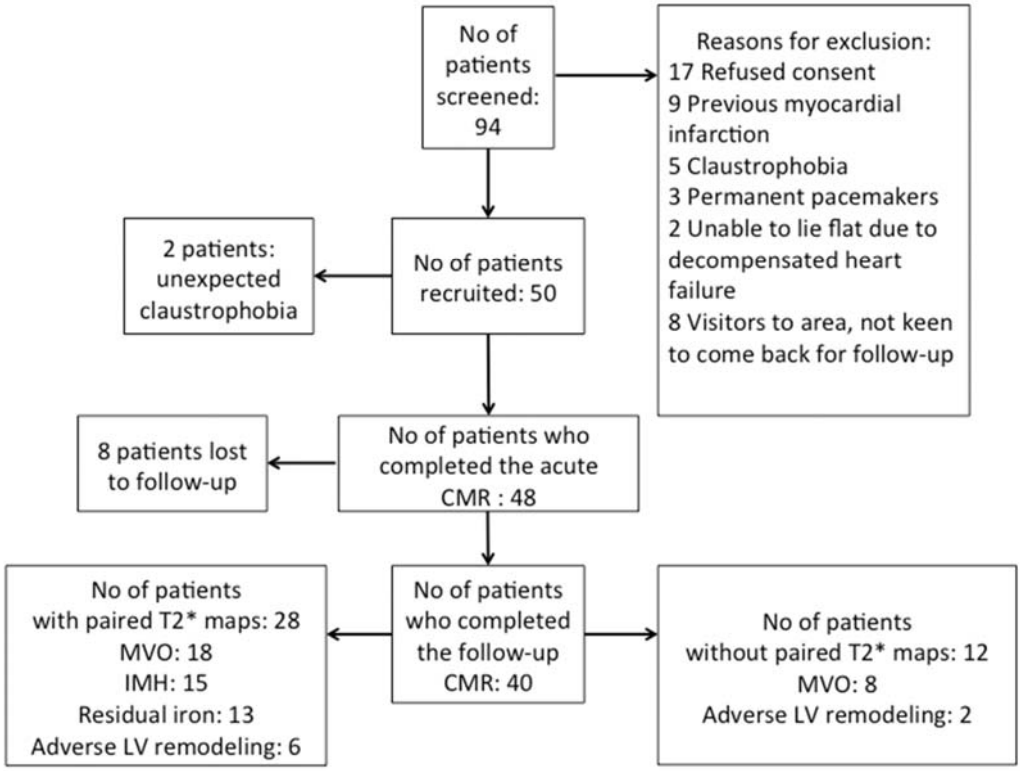

Supplemental Table: CMR characteristics patients with and without paired T2* maps

	Patients with paired T2* maps (n=28)	**Patients without paired T2* maps (n=12)**	**P value**
EDV/ml	173±40	170±31	0.79
ESV/ml	91±32	87±24	0.71
EF/%	48±9	50±7	0.58
Mass/ g	119±33	104±24	0.15
Change in EDV/ ml	7±16	3±13	0.44
Acute infarct size/ %LV	26.7±15.2	28.8±13.6	0.69
Follow-up Infarct size/ %LV	18.5±11.1	22.0±9.8	0.36
T2-based AAR/ % of LV	42.7±12.3	40.3±11.8	0.56
MVO/ n (%)	18 (64)	8 (67%)	0.59
Adverse LV remodeling/ n (%)	6 (21%)	2 (17%)	0.55
Acute scan			
$T2_{Remote}$	50 (48-52)	50 (48-52)	0.85
$T2_{Core}$	52 (48-55)	51 (48-54)	0.96
$T2_{Infarct}$	64 (62-68)	65 (64-66)	0.80
Follow-up scan			
$T2_{Remote}$	48 (46-50)	47 (45-49)	0.63
$T2_{Core}$	47 (45-49)	47 (46-48)	0.90
$T2_{Infarct}$	57 (53-61)	54 (52-57)	0.25